

Electroretinography and optical coherence tomography reveal abnormal post-photoreceptor activity and altered retinal lamination in patients with enhanced S-cone syndrome

M. Sustar · D. Perovšek · I. Cima ·
B. Stirn-Kranjc · M. Hawlina · J. Breclj

Received: 30 June 2014 / Accepted: 26 January 2015 / Published online: 7 February 2015
© Springer-Verlag Berlin Heidelberg 2015

Abstract

Purpose To compare functional abnormalities of enhanced S-cone syndrome (ESCS), as examined using standard and extended electroretinography (ERG), with structural findings and retinal architecture obtained by spectral domain optical coherence tomography (SD-OCT).

Methods Four patients with ESCS underwent standard full-field and multifocal ERGs, with extended S-cone and ON/OFF ERG protocols also performed. SD-OCT was also carried out, and longitudinal reflectivity profiles (LRPs) were calculated for the perifoveolar retina.

Results All four patients exhibited pathognomonic full-field ERG findings for ESCS, with delayed responses of similar waveforms to the same intensity flash under both scotopic and photopic conditions. The amplitudes of the full-field ERGs showed considerable variation between patients, which were not related to the extent of the visual field defects. Multifocal ERGs reflected preserved central function in eyes with good visual acuity (Snellen visual acuity >0.7). The ERGs to S-cone-specific stimulation confirmed the expected

predominant activity of the S-cone system in all four patients. The ON/OFF ERG recordings revealed abnormal presence of both ON-response and OFF-response activities in three patients; the remaining patient showed only OFF-response activity. SD-OCT showed a significantly thickened outer nuclear layer in all four patients, as obtained by LRP analysis. Furthermore, in the patient with selective preservation of the OFF-response activity, LRP showed reduced numbers of hyper-reflectivity sub-peaks in the inner plexiform layer.

Conclusion Patients with ESCS show characteristic full-field ERG waveform abnormality, predominance of S-cone ERG activity, and thickening of the outer nuclear layer on SD-OCT. Moreover, they can also show abnormal post-photoreceptor connectivity through S-cone-related OFF-bipolar cell activity.

Keywords Enhanced S-cone syndrome · Longitudinal reflectivity profile · NR2E3 · OCT · ON- and OFF-responses · S-cone ERG

M. Sustar (✉) · D. Perovšek · B. Stirn-Kranjc ·
M. Hawlina · J. Breclj
Eye Hospital, University Medical Centre,
Grablovičeva 46, 1000 Ljubljana, Slovenia
e-mail: sustar.majchi@gmail.com; maja.sustar@kelj.si

I. Cima
Eye Clinic Sörmland, Mälarsjukhuset, Eskilstuna, Sweden

Introduction

Enhanced S-cone syndrome (ESCS) is an autosomal recessive retinal disorder that is characterized by night blindness from an early age, variable loss of visual acuity, and increased sensitivity to blue light [1, 2]. ESCS is caused by mutations in the *NR2E3* gene,

which encodes a retinal orphan-photoreceptor-specific nuclear receptor [3, 4]. The pathogenic mechanism of the mutation is not clearly understood. However, it appears that the NR2E3 protein has a key role in rod and cone photoreceptor development and maintenance, as it appears to act as a suppressor of the cone generation program in retinal progenitor cells and as a transcriptional activator of several rod-specific genes, including rhodopsin [5]. The retina of ESCS patients contain no rod photoreceptors, and most of the cones are the short-wavelength-sensitive type (S-cones), while long-wavelength- and medium-wavelength-sensitive cones (L-/M-cones) are degenerate to various degrees [6]. Mutations of the *NR2E3* gene have also been identified in related retinal disorders, including Goldmann-Favre syndrome, clumped pigmentary retinopathy, and autosomal dominant retinitis pigmentosa [5, 7].

Functional defects in ESCS patients can be identified by pathognomonic features of electroretinograms (ERGs), in which responses to shorter wavelengths of light are relatively increased [1], the waveform to the same strength of flash is similar under both photopic and scotopic conditions, and there is a loss of the rod response b-wave elicited with dim scotopic flash (dark-adapted 0.01 ERGs) [8, 9]. Although these ERG features are well established, large variations in the response amplitudes are still intriguing. The full-field ERG amplitude in molecularly confirmed ESCS varies from abnormally large [9] to severely reduced [10], and there are even cases with very mild functional impairment and preserved rod function [11, 12]. However, amplitude variations might partly relate to disease progression. The multifocal ERG abnormalities in ESCS have not been studied extensively. To our knowledge, there has been only one detailed multifocal ERG study, which showed differences between central and peripheral multifocal ERG responses in one patient with ESCS [13]. Extended ERG protocols previously showed the expected S-cone-related ON-bipolar cell activity and also indicated OFF-bipolar cell activity in some, but not all, patients with ESCS [8, 14, 15]. This S-cone-related OFF-bipolar activity was suggested to be the result of abnormal second-order retinal development [8], as the S-cone typically only connects to ON-bipolar cells [16].

Structural impairment of the ESCS retina has also been reported [6, 17, 18]. Histopathology of the

postmortem retina of one older patient with ESCS identified lack of structurally recognizable rods, increased number of S-cones, and disorganized retina, with cones intermixed with inner retinal neurons [6]. Optical coherence tomography (OCT) showed thickened retinal layers within an otherwise normally structured retina in early stages of the disease. In later stages, retinal lamination was coarse, with a thick and bulging appearance of the retina, localized to an annulus encircling the central fovea [17]. Cases with normal overall retinal structure and thinner retina have also been described [19].

The aim was to examine the phenotypes in a series of four genetically confirmed cases of ESCS. Retinal function was characterized using extended ERG protocols that included ON/OFF ERGs and S-cone ERGs, and perifoveal structure was detailed using longitudinal reflectivity profiles (LRPs) and retinal thickness maps based on spectral domain OCT.

Subjects and methods

This study was performed according to the tenets of the Declaration of Helsinki, and it was approved by the National Ethics Committee. All of the subjects provided their signed approval for study participation, and they were fully informed of the study protocol.

Four patients with ESCS (one female, three males) aged 31–49 years participated in this study. Early standard full-field ERG findings of two of these patients (ESCS-2, ESCS-3) have been described previously in a larger international study of ESCS patients [8], and one patient (ESCS-4) was recently the subject of a case study [20]. The S-cone-specific ERGs of all four of these patients have been previously used for identification of optimal stimulus conditions to elicit S-cone responses [21]. However, the structural findings and their correlation with extended electroretinography have not been investigated previously in these patients. The data of 20 control subjects (aged 24–59 years) were also analyzed, to obtain confidence limits for the structural OCT parameters. As an exemplary comparison, structural findings of four male patients (aged 15–19 years) with complete type of congenital stationary night blindness (complete CSNB) are presented in this study. The clinical and electrophysiological findings of complete CSNB patients are described in detail elsewhere [22, 23].

The ophthalmological examination included best-corrected visual acuity according to the Snellen chart (decimal units), slit-lamp and dilated fundus examination, and visual field analysis with Octopus automated static perimetry (TOP strategy, program tG2). Mutational screening for the *NR2E3* gene was also carried out and confirmed the *NR2E3* mutation in all four of these patients.

The ERGs were recorded simultaneously from both eyes. The recording electrode was an HK loop that was placed in the fornix of the lower eyelid [24]. The silver chloride reference electrode was placed on the ipsilateral temple, and the ground electrode was positioned on the forehead. The pupils were dilated with 1 % tropicamide (Mydracyl[®], Alcon, Belgium). The recording of the full-field and multifocal ERGs followed the standards of the International Society of Clinical Electrophysiology of Vision [25, 26].

Full-field ERG was performed using a Ganzfeld stimulator of the RETI port unit (Roland Consult, Wiesbaden, Germany). Dark-adapted ERG responses (dark-adapted 0.01 ERGs, dark-adapted 3.0 ERGs, and dark-adapted 3.0 oscillatory potentials) were obtained after 20 min of dark adaptation. Light-adapted ERG responses (light-adapted 3.0 ERGs, light-adapted 3.0 flicker ERGs) were obtained after 10 min of light adaptation, at a background luminance of 30 cd/m². The luminance of the standard flash was 3 cd s/m², and the luminance of the attenuated dark-adapted flash was 0.01 cd s/m². For dark-adapted responses, eight sweeps were averaged for each recording, while for light-adapted responses, 30 sweeps were collected and the measurement was repeated at least twice.

Multifocal ERGs were recorded using the RETI scan system (Roland Consult, Wiesbaden, Germany) with a field diameter of 60° (61 hexagons), to examine a wider area of macular region. The stimulus was at a distance of 260 mm, and refractive errors due to cycloplegia were corrected with +3.50 diopters. The recording sessions consisted of eight trials that lasted 50 s each.

S-cone ERGs were elicited with a Ganzfeld Espion ColorDome stimulator (Diagnosys LLC, Littleton, MA, USA) with 0.016, 0.063 and 0.25 cd s/m² blue (449 nm) stimuli on a 100 cd/m² amber (594 nm) background. The flashes were generated with a xenon bulb, and a blue filter was placed between the bulb and the patient (Wratten

47B; radiance peak, 449 nm). For each recording, 15 sweeps were averaged and the measurement was repeated at least twice.

ON-OFF ERGs were elicited with a ColorBurst light-emitting diode (LED) stimulator (Diagnosys LLC, Littleton, MA, USA) with broadband white (strength, 1.7 log cd s/m²; wavelength composition, blue 651 nm, green 511 nm, red 650 nm LEDs; color temperature 6,500 K) and monochromatic blue (461 nm LED; strength, 1.7 log cd s/m²) stimuli on a white background (40 cd/m²). The flash duration was 200 ms. The strengths of the flashes were set to the same photopic luminance, to achieve equal stimulation of the L-cone and M-cone mechanisms. In this way, differences in the response amplitudes between the white and blue flashes were interpreted as the consequence of the S-cone system activity. For each response, 20 sweeps were averaged and the measurement was repeated at least twice. All of the responses were differentially amplified and stored on the hard disk of a computer. The flash and background luminance were calibrated with a photometer/radiometer (IL-1700, International Light INC, Newburyport, USA), using detectors with integrated photopic and scotopic filters.

SD-OCT scanning of the macula was performed with a Topcon 3D OCT-1000-Mark II instrument (Topcon, Tokyo, Japan). The superluminescent diode light source used was centered at 850 nm with a bandwidth of 50 nm. Retinal lamination was further studied with LRPs. The methodology for the LRP calculations was similar to that described in detail in previous studies [17, 27, 28]. The cross-sectional RGB retinal image through the foveolar region was exported, and a slice of the temporal perifoveolar retina was chosen for further analysis (taken from 2.2 to 2.8 mm perifoveolarly; total width of cross sections analyzed, 0.6 mm). This region was chosen according to the best preservation of function among all of the patients and to avoid regions of notable intraretinal schisis. Post-acquisition processing was first performed in the Adobe[®] Photoshop[®] CS3 program, where the OCT scan was manually aligned. Within this selected 0.5-mm image, 170 parallel LRPs were calculated with the OriginPro 8.1 program (OriginLab, Northampton, USA). These 170 LRPs were averaged, and the signal intensity was normalized to provide relative LRP values. The diameters of the hyper-reflectivity and hypo-reflectivity layers were measured manually as the longitudinal distances

between the midpoints of each reflectivity peak or trough. The retinal structures were comparatively evaluated, according to the 5–95 % confidence limits of the age-matched control group.

Results

Four patients with ESCS were identified during routine clinical and electrophysiological examinations at the University Eye Hospital, Ljubljana (Slovenia). At the time of inclusion, the patients showed various decreases in their Snellen visual acuity and a history of night blindness since childhood. Their visual fields were considerably constricted. Clinical examination revealed nummular pigmentation around the vascular arcades in all four of these subjects, and areas of chalky white preretinal reticular deposits were seen in patient ESCS-4. Disrupted macular structure was also seen. Their clinical findings and molecular details (*NR2E3* mutations) are given in Table 1.

Full-field and multifocal ERG abnormalities

The full-field ERGs in all four of the patients showed characteristic findings for ESCS (Fig. 1). Dark-adapted 0.01 ERGs (rod system responses) were not

detectable, while dark-adapted 3.0 ERGs (combined rod-cone responses) and light-adapted 3.0 ERG (cone responses) were simplified and delayed and had similar waveforms. The light-adapted 3.0 flicker ERGs were delayed and of lower amplitude than the cone response a-waves. The implicit times of the full-field ERG responses were delayed in all of the patients, while the amplitudes of the responses had a wider range of abnormality, from moderate amplitude abnormality in patient ESCS-1 to the most severe amplitude reduction in patient ESCS-4. Furthermore, the extent of the full-field ERG amplitude abnormality did not relate to visual field disturbances. This was most clearly seen in two of the patients. Patient ESCS-1 had the most extensive visual field defect, with the largest ERG amplitudes, while patient ESCS-4 had the best preservation of visual field, but the most severely reduced ERG amplitudes.

Multifocal ERG was recorded for the evaluation of central retinal function (Fig. 2). The distribution of the multifocal ERGs showed preservation of responses for up to approximately 15° of the central retina, which corresponded with the first three rings, while the responses in the peripheral rings were either reduced or absent. The central P1 response of the multifocal ERG appeared to be related to visual acuity, as it was preserved in the left eye of patient ESCS-3 and in the

Table 1 Clinical characteristics of the four ESCS patients in the present study

Patient code	Age	Sex	<i>NR2E3</i> mutation	Visual acuity	Visual field			OCT findings
					Appearance	MD	LV	
ESCS-1	49	M	c.119-2A > C c.1049A > G	Re: 0.1	Constriction, preserved central 5°–7°, ↓ sensitivity	16.3	50.8	Large intraretinal schisis
				Le: 0.2	Constriction, preserved central 4°–6°, ↓ sensitivity	14.7	61.4	Abnormal foveolar structure
ESCS-2	31	M	c.481delA c.481delA [8]	Re: 0.3	Constriction, preserved central 7°–13°	18.6	73	Abnormal foveolar structure
				Le: CF	Constriction, preserved central 14°	17.4	80.7	Preserved macular appearance
ESCS-3	33	M	c.481delA c.481delA [8]	Re: 0.2	Constriction, preserved 5°–15°, central scotoma	16.3	69.3	Large intraretinal schisis
				Le: 0.7	Constriction, preserved central 5°–15°	16.5	62.9	Small macular cysts, preserved lamination
ESCS-4	43	F	c.481delA c.1120C > T [20]	Re: 0.9	Constriction, preserved central 12°–15°	14.6	59.4	Preserved macular structure
				Le: 1.0	Constriction, preserved central 13°–15°	13.4	69.4	Preserved macular structure

M male, *F* female, *Re* right eye, *Le* left eye, *MD* mean defect [dB], *LV* lost variance

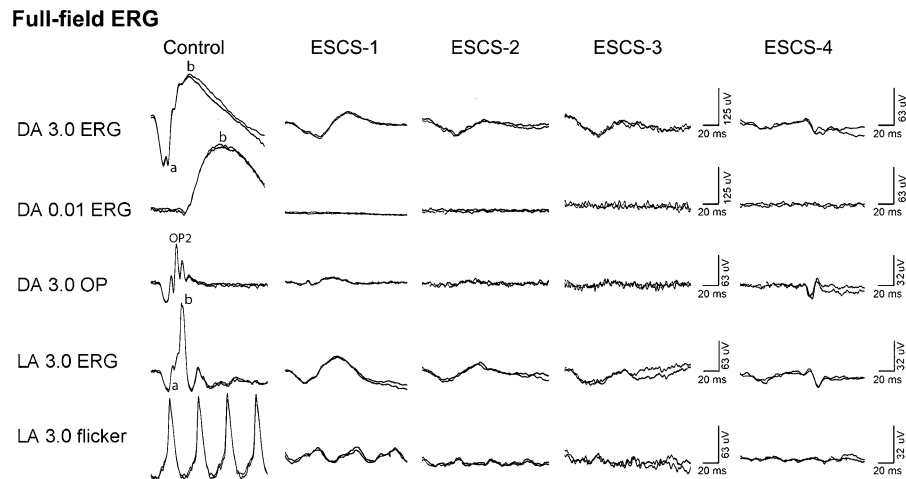


Fig. 1 In the four patients in the present study, the standard full-field ERGs show characteristic abnormalities. The full-field ERG traces are symmetrical for both eyes, and therefore, the responses from only one eye for each patient are shown. *DA* dark adapted, *LA* light adapted. Dark-adapted 3.0 ERGs (combined

rod-cone responses); dark-adapted 0.01 ERGs (rod system responses); dark-adapted 3.0 oscillatory potentials; light-adapted 3.0 ERGs (cone responses); light-adapted 3.0 flicker (30 Hz flicker). Two waveforms are superimposed to demonstrate reproducibility

both eyes of patient ESCS-4, which also showed preservation of visual acuity ($VA > 0.7$). In contrast, in the eyes with decreased visual acuity ($VA < 0.7$), the central response was reduced in comparison with the averaged response of the second ring in patients ESCS-1 and ESCS-2, as well as in the right eye of patient ESCS-3, in which the central response was within the noise level. However, the possibility of fixation error and its impact on the multifocal ERG amplitude cannot be completely excluded.

Function of the S-cone mechanism and activity of the ON- and OFF-response retinal pathways

S-cone ERGs to blue stimuli were used to evaluate the function of the S-cone mechanism (Fig. 3a). To characterize the responses of the S-cone system, the luminance of the S-cone-specific stimulus was gradually increased. In control subjects, the predominant activity of the S-cone mechanism is identified only with the dimmest strengths of blue flash (0.016 cd s/m^2), in which the responses showed simple, monophasic waveforms. With brighter flashes (0.063 cd s/m^2), typical responses showed a biphasic appearance, as well as the S-cone component, and there was interference of the faster L-cone and M-cone components. With the brightest blue stimulus (0.25 cd s/m^2), the L-cone and M-cone components predominated in the

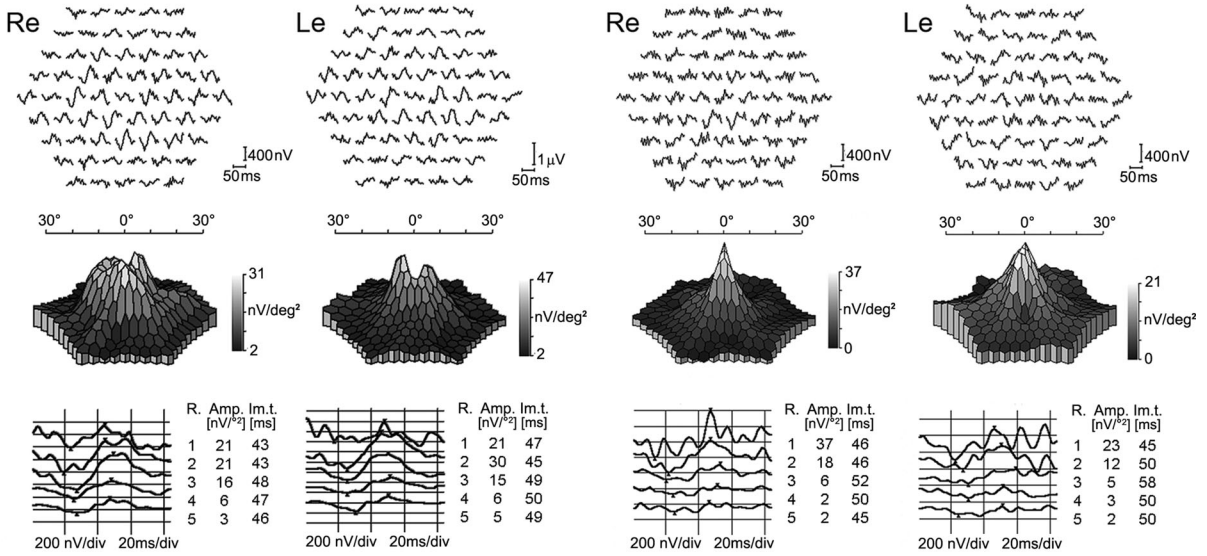
response. This typical course of waveform changes with the S-cone-specific stimuli due to the S-, M- and L-cone mechanisms was previously described in detail elsewhere [21]. In contrast, in all four of these patients with ESCS, their responses to S-cone-specific stimulation showed simple, monophasic and delayed waveforms to all of these flash strengths. These responses were larger and considerably more delayed than the normal S-cone responses (Table 2). The waveforms of the S-cone responses in the patients with ESCS were essentially similar to those of the combined rod-cone responses and the light-adapted cone responses. However, their amplitudes to the brightest S-cone-specific stimuli were larger, although they were elicited at considerably lower flash strengths (S-cone-specific stimuli, 0.25 cd s/m^2 ; standard full-field ERGs, 3 cd s/m^2), which indicated that the majority of the ERG responses were broadly consistent with an S-cone mechanism of origin.

The responses to long-duration stimuli were used to evaluate the function of the retinal ON- and OFF-response bipolar cell mechanisms (Fig. 3b). In control subjects, the ON-response comprised two prominent waves, the negative a-wave and the positive b-wave, whereas the OFF-response was the positive d-wave. Furthermore, with white and with blue stimuli, the response waveforms remained identical in the control subjects, due to the weighted equal stimulation of the

Multifocal ERG

ESCS-1

ESCS-2



ESCS-3

ESCS-4

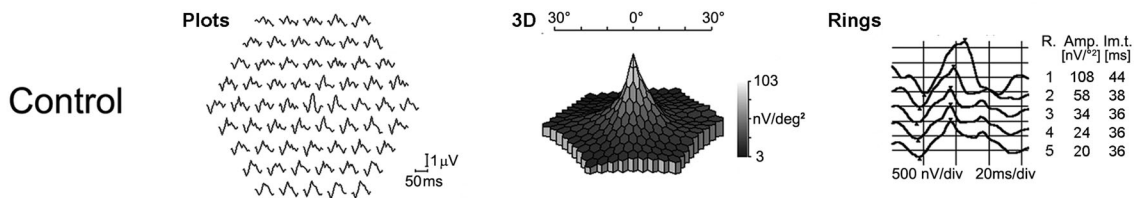
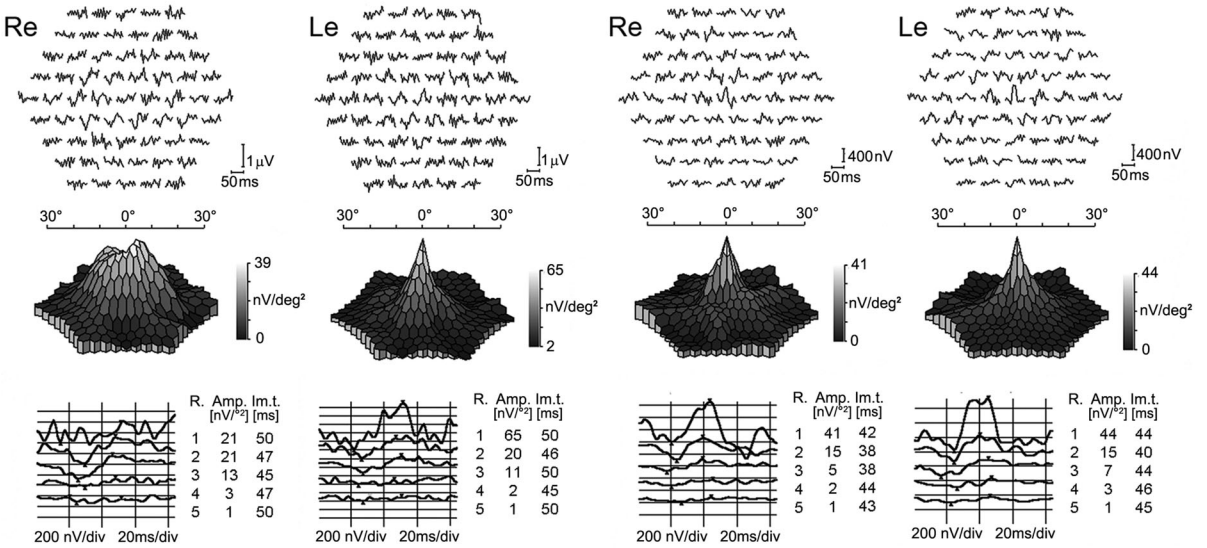


Fig. 2 Multifocal ERGs from the patients with ESCS, showing various degrees of macular involvement. The multifocal ERGs are presented for both eyes: *Re* right eye, *Le* left eye, *R. rings*, *Amp.* amplitude; *Im.t.* implicit time

Fig. 3 In the four patients in the present study, the S-cone-specific ERGs are relatively increased (A), and long-duration stimuli a- and d-waves could be elicited in all four patients, while the b-wave is absent in one patient (B). Two waveforms are superimposed to demonstrate reproducibility

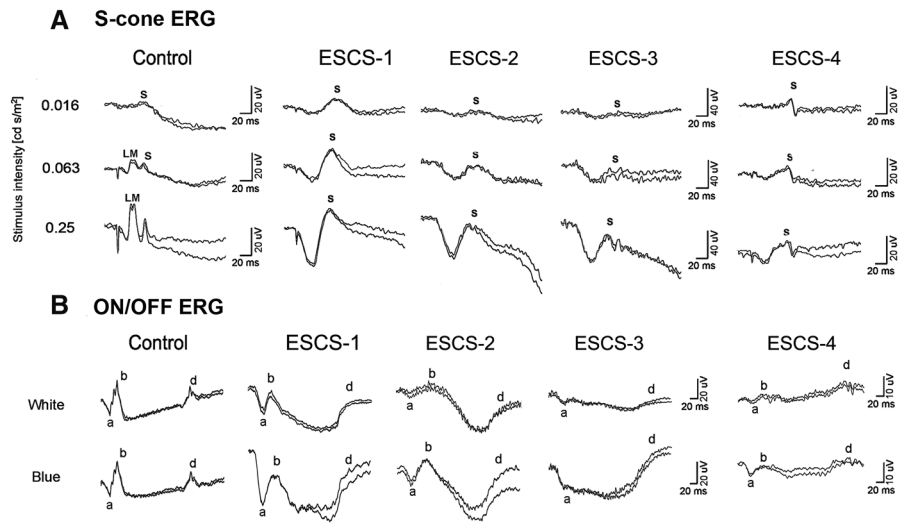


Table 2 Summary of the functional and structural findings of the four patients in the present study

Patient	Eye	DA 3.0 ERG		MFERG	Extended ERG		OCT		LRP	
		A-wave [μV; ms]	B-wave [μV; ms]	PI [nV; ms]	S-cone ^a [nV; ms]	ON/ OFF ^b	TV [μm]	CT [μm]	ONL [μm]	IPL
ESCS-1	Re	74; 33	129; 59	21.4; 43	25; 68	ON/OFF	13.1	920	127.8	3 peaks
	Le	62; 31	100; 59	21.3; 47	22; 65		8.0	203	117.9	
ESCS-2	Re	46; 34	46; 61	37.1; 46	10.; 75	ON/OFF	7.1	142	103.7	3 peaks
	Le	46; 35	36; 63	23.0; 45	13; 76		7.5	235	97.8	
ESCS-3	Re	54; 35	46; 61	21.4; 50	15; 82	OFF only	10.8	714	114.5	2 peaks
	Le	52; 37	38; 63	65.4; 50	15; 79		9.7	219	144.6	
ESCS-4	Re	8; 27	15; 58	41.1; 42	7; 63	More ON	8.3	208	99.5	Multiple peaks
	Le	13; 27	17; 58	43.7; 44	9; 65		8.2	223	106.3	
Normal range [5–95 %]		92–191; 20–24	169–347; 42–58	92–172; 35–44	1.8–10; 37–55		7.1–8.0	165–235	73–88	3 peaks

^a S-cone response elicited with 0.016 cd s/m² stimuli, as used in the routine clinical extended ERG protocol

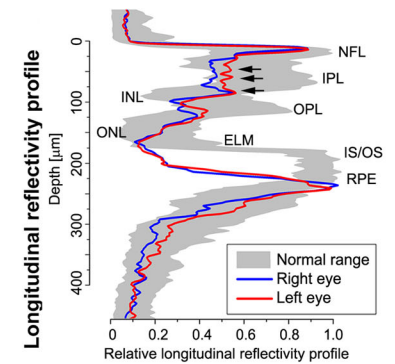
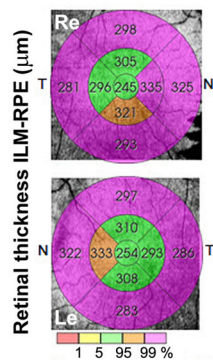
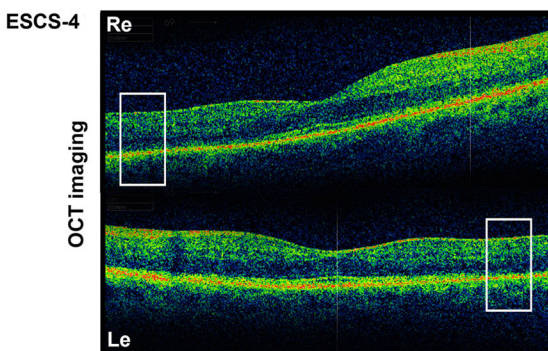
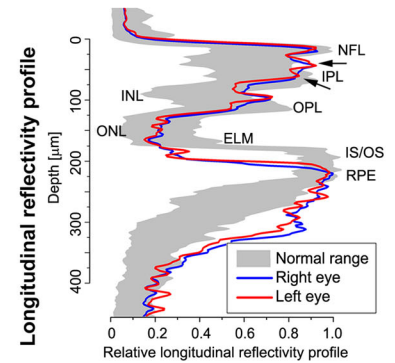
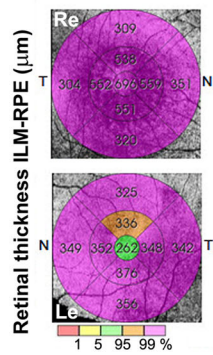
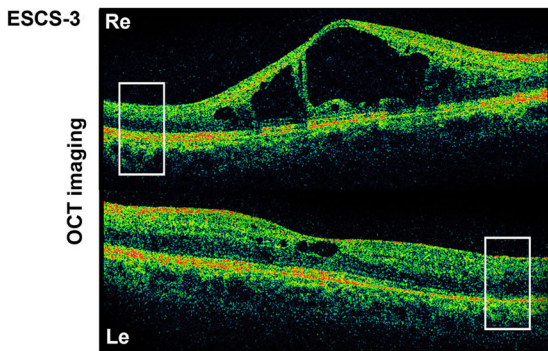
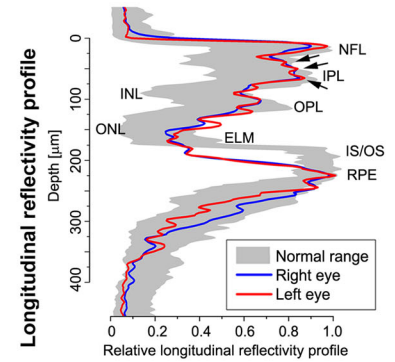
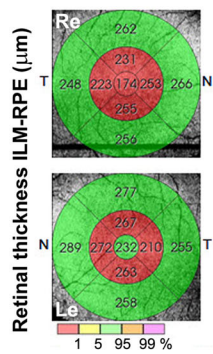
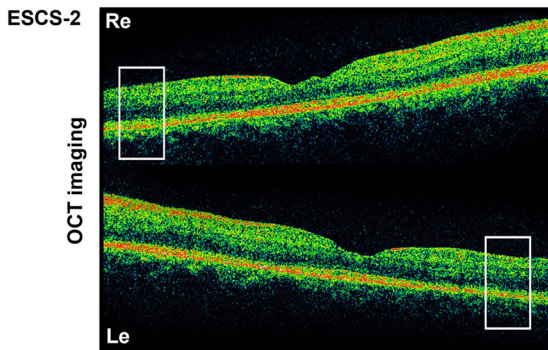
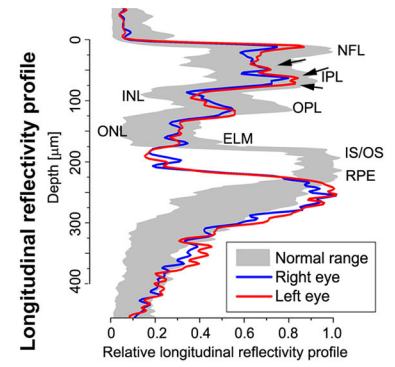
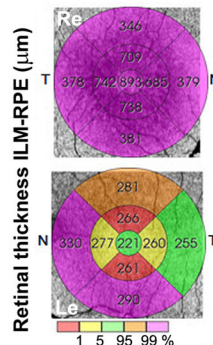
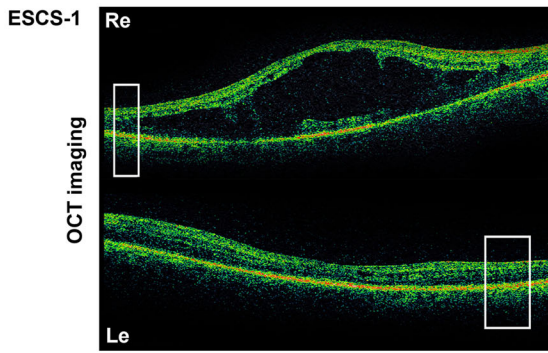
^b ON-responses and OFF-responses to S-cone-specific stimulation

predominant L-cone and M-cone mechanisms. In patient ESCS-1, a-, b- and d-waves were present, but the waveforms were different from normal, with a delayed implicit time and a sustained waveform for the d-wave. With blue stimuli, there was an enlargement of all three waves compared with white flash responses. Patient ESCS-2 showed similar findings as patient ESCS-1. In patient ESCS-3 (brother of patient ESCS-2), a- and d-waves were clearly recognizable, while the b-wave was small and almost extinguished to white flashes. With blue flashes, the amplitudes of a- and d-waves were increased, while the b-wave was

seen only as a possible residual response. In patient ESCS-4, the white flash ON/OFF ERG a-, b- and d-waves were markedly reduced and b- and d-waves were of similar low amplitude. The blue flash elicited larger a- and b-waves, but there was no corresponding increase in the d-wave.

Morphological findings with SD-OCT and LRP analysis

Visual inspection of the cross-sectional SD-OCT images in patient ESCS-1 (Fig. 4) revealed large



◀ **Fig. 4** SD-OCT macular scans of the four patients with ESCS, and their corresponding retinal thickness maps and LRPs. The white frames on the OCT scan approximate the retinal region taken for the LRP analysis (2.2–2.8 mm of temporal perifoveolar retina). Discrete LRP peaks that correspond to anatomical layers of the OCT are marked for the normal range: *NFL* neural fiber layer, *IPL* inner plexiform layer, *INL* inner nuclear layer, *OPL* outer plexiform layer, *ONL* outer nuclear layer, *ELM* external limiting membrane, *IS/OS* inner/outer segment photoreceptor layer, *RPE* retinal pigment epithelium, arrows hyper-reflectivity sub-peaks inside the IPL. Black arrows hyper-reflectivity sub-peaks at the inner plexiform layer (IPL)

intraretinal schisis (diameter, 5 mm), with delamination of the foveolar retina at the level of the outer nuclear layer (ONL) in the right eye. In the left eye, the foveolar structure was preserved. In both eyes, there was partial diffuse loss of the photoreceptors, which was seen as loss of the inner segment/outer segment (IS/OS) junction and thinning of the retinal nerve fiber layer (RNFL). The thickening of the retina was notable in both eyes, which was more severe in the right eye, due to the presence of a large macular cyst (Fig. 4; Table 2). In patient ESCS-2, the foveolar laminar structure was preserved, along with a slightly diminished foveolar topography. Retinal thickness was within normal limits in both of the eyes, although slight thinning was detected at the perifoveolar annulus (Fig. 4; Table 2). In contrast, patient ESCS-3 (the brother of patient ESCS-2) had intraretinal cysts in both eyes, with larger intraretinal schisis in the right eye (diameter, 3.5 mm), as well as delamination of the foveolar retina. In regions without schisis, the retinal lamination was preserved, although there was slight diffuse photoreceptor deterioration. The retina of patient ESCS-3 was thicker than normal, which was

also notable in the perifoveolar regions, where no apparent schisis could be identified. In patient ESCS-4, no foveal cystoid changes or retinoschisis were seen in either eye, and retinal thickness was also notably increased in the perifoveolar regions.

Quantification of retinal lamination was performed using LRP (Figs. 4, 5; Table 2). A region of the perifoveolar retina was chosen for analysis, as in this region, retinal function was relatively preserved in most patients (according to the multifocal ERG and visual field testing), and no intraretinal schisis was present in the analyzed slice. In the control subjects, LRPs appeared as layers with different amplitudes of signal, in which the hypo-reflective layers corresponded to the inner and outer nuclear layer, while hyper-reflectivity matched with the synaptic layers. At the inner plexiform layer (IPL), three hyper-reflective sub-peaks were observed in all of the control subjects. Patient ESCS-1 showed preserved retinal lamination through the LRP profiling. In agreement with the visual inspection of the OCT, the LRP also showed a diminished photoreceptor IS/OS peak and a relatively thin RNFL, while the most profound finding was considerable thickening of the ONL. The three hyper-reflective sub-peaks in the IPL were similar to those seen in the controls (Fig. 5). In patients ESCS-2 and ESCS-3, retinal lamination was preserved, the photoreceptor IS/OS peaks were diminished, and the ONL was thickened (Table 2). However, there was a difference in the reflectivity profile between the patients ESCS-2 and ESCS-3 at the level of the IPL. In patient ESCS-2, three hyper-reflective sub-peaks were identified, and they appeared similar to those of patient ESCS-1 and the control subjects. In patient ESCS-3,

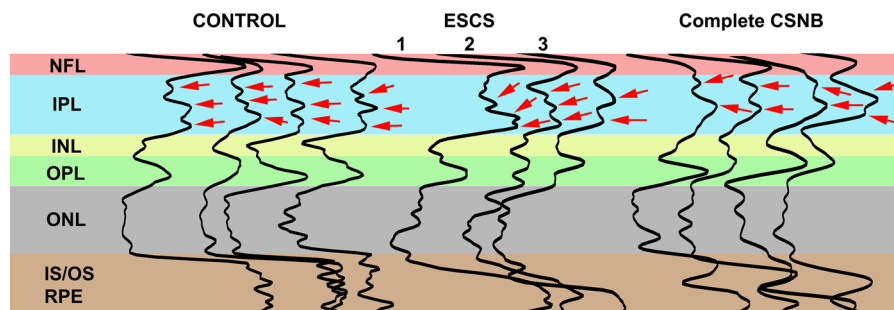


Fig. 5 Comparison of relative LRPs of four control subjects, three patients with ESCS, and with an example also of four patients with complete CSNB. LRPs are vertically rescaled to match the anatomical levels of the OCT: *NFL* neural fiber layer,

IPL inner plexiform layer, *INL* inner nuclear layer, *OPL* outer plexiform layer, *ONL* outer nuclear layer, *IS/OS* inner/outer segment photoreceptor layer, *RPE* retinal pigment epithelium, arrows hyper-reflectivity sub-peaks inside the IPL

the IPL showed only two hyper-reflective sub-peaks, which were shifted toward the RNFL in such a way that the hypo-reflective band between the IPL and the RNFL hyper-reflectivity was extinguished. In patient ESCS-4, the retinal lamination of the LRP was in general preserved, with profound thickening of the ONL, while peaks at the IPL could not be reliably discriminated from the noise level (Fig. 4).

To further characterize a lack of hyper-reflectivity sub-peaks in patient ESCS-3, LRP findings (Fig. 5) were observed in four patients with complete type of congenital stationary night blindness (complete CSNB). This group of patients was chosen according to the characteristic selective preservation of the OFF-response (d-wave) ERG activity, which was found also for patient ESCS-3. In complete CSNB patients, LRP showed only two hyper-reflectivity sub-peaks in the IPL, which appeared similar to patient ESCS-3.

Discussion

The present study of four cases with ESCS describes the functional and structural characteristics of this rare retinal disorder. The common findings in all four patients were characteristic full-field ERG abnormality [8], predominance of S-cone ERG activity [1], and thickening of the ONL on the OCT [17]. S-cone-related ON-response activity was detectable in three patients, while OFF-response activity was identified in all four patients. In a patient with selective preservation of the retinal OFF-response, this functional abnormality appeared to be associated with a reduced number of hyper-reflectivity sub-peaks at the IPL. This finding might indicate that primarily photoreceptor disease leads to abnormal post-photoreceptor connectivity independent of its genotype, as the ERG and SD-OCT findings were different in a sibling who was homozygous for the same *NR2E3* mutation.

All four patients in this series were selected on the basis of confirmed *NR2E3* mutation, pathognomonic changes in the ISCEV-standard ERGs and predominance of S-cone ERG activity, described in several previous publications [1, 2, 8, 14, 29, 30]. However, the present study also defines a common structural abnormality that was present in all four of these ESCS patients and was seen as a thickening of the ONL on the OCT. The thickening of the ONL has been described previously in only one study, by

Jacobson et al. [17], in a group of 17 patients. Other OCT studies have described cystic changes in the macula as the most common finding in ESCS [8, 11, 18, 31, 32]. Disorganized retinal lamination with splitting at the level of the outer retinal layers [18] or normal overall retinal structure within thinner retina have also been described [19]. In the present study, there were cystic changes in only half of the patients; the retina was thicker than normal in three patients, and the retinal lamination in the central regions was in generally preserved, while profound thickening of the ONL was common in all four of these patients. This was seen also in the case when the overall retinal thickness was normal. Therefore, it is possible that ONL thickening presents a common structural alteration of the retina in patients with ESCS.

Large variability of full-field ERG amplitudes in patients with ESCS was previously not explained. In the present study, the ERG amplitude abnormalities did not correlate with psychophysically measured visual field disturbances. This can be identified also from other studies, where cases with relatively good preservation of the visual field show severely reduced ERG amplitudes [7], or the ERG amplitudes are inconsistently variable in patients who share similar degrees of visual field abnormality [33]. It is therefore possible that the amplitudes of full-field ERGs in ESCS might not be primarily related to the extent of retinal dysfunction, but might rather reflect variously responsive retinal cells inside the functional part of the retina. Multifocal ERG findings in our patients were in agreement with this hypothesis, as they showed preservation of the responses to approximately within 15° of the central retina, which is comparable to the results of visual field testing, while their amplitudes were affected to a relatively similar degree, as seen with the full-field ERGs. However, ERG amplitude and the results of visual field testing do not necessarily correlate, as the visual fields test threshold sensitivity and the ERGs test suprathreshold activity.

Although ESCS is primarily a photoreceptor disorder, abnormal post-photoreceptor connectivity was previously assumed [8, 14, 15]. Post-photoreceptor activity can be more precisely evaluated with responses to long-duration stimuli that can separately evaluate the functions of the ON-bipolar cells *versus* the OFF-bipolar cells [34–37]. Studies in non-human primates have reported that the a-wave originates from cones and partially also from post-photoreceptor activity,

mainly from OFF-bipolar cells [34]. The b-wave origin has been related to the ON-bipolar cells, although its amplitude and shape have been shown to be influenced by OFF-bipolar and horizontal cells [35, 36]. Studies of the d-wave origin have demonstrated that the initial phase of the d-wave originates from OFF-bipolar cells and cones that contribute to the later phases, while the amplitude and shape are modulated by ON-bipolar cells [37]. In healthy retinas, S-cones are only connected to ON-bipolar cells [16, 38]. In patients with ESCS, previous studies have shown not only an expected ON-bipolar cell activity, but in some cases, also measurable OFF-bipolar cell activity [8, 14]. Similar to previous studies, two of our patients had clearly recognizable both ON-response b-waves and OFF-response d-waves to S-cone-specific stimuli. In one patient (ESCS-3), the findings were exceptional, because this patient showed a predominance of the OFF-response d-wave, which became even more prominent to blue S-cone-specific stimulation, while the b-wave was seen only as a possible residual response. Previously, Román and Jacobson [14] noted that a measurable OFF-response might not necessarily represent an abnormal S-cone to OFF-bipolar cell connectivity; instead this might also be a false OFF-effect due to the algebraic sum of the various waveform components. For instance, it might represent cone activity and its return to baseline. Another argument against the presence of OFF-bipolar cell activity in ESCS would be the possible contamination with the blinking artifacts. However, this cannot be the case, because the same delayed and sustained waveform of the d-wave has been described before in ESCS [8, 14]; also, the waveforms in the present study showed good reproducibility. Our results cannot completely exclude a primarily photoreceptor origin of the observed d-wave. However, as there was no b-wave and the only possible post-photoreceptor transmission in this patient was through the activity related to the d-wave, these findings most likely indicate that the S-cones to OFF-bipolar cell connections are truly present in ESCS retinas, which indicates abnormal development of second-order retinal connectivity.

Furthermore, an interest of present study was to determine whether there were any structural correlates with the abnormal post-photoreceptor connectivity in our group of ESCS patients. It was previously shown by Tanna et al. [39] that sublamination and synaptic

aggregation of the IPL of the retina might be seen through three distinct hyper-reflective sub-peaks at the level of the IPL. These hyper-reflective sub-peaks were identified in all of our control subjects. At the level of the IPL, bipolar cells form synapses with corresponding ganglion and amacrine cells. Anatomically, the IPL is divided into two functionally discrete sublaminae, which separate the ON-channels and OFF-channels of the bipolar-to-ganglion cell contacts [40, 41]. The appearance of discrete peaks inside the IPL might therefore correspond to these histological sub-layers; however, additional histological evidence will be needed to confirm this finding. In the present study, three hyper-reflective sub-peaks at the IPL were seen also in the two ESCS patients who showed functionality for the ON- as well as OFF-bipolar cell activities. However, the patient with the functional disruption of the ON-bipolar cell pathway showed only two discrete hyper-reflective sub-peaks of the IPL. It is possible that these two findings correspond and that the developmental lack of otherwise normal S-cones to ON-bipolar cell connectivity might be structurally seen as a lack of sublaminae at the IPL. In agreement with this hypothesis, our findings in patients with a complete type of CSNB that was electrophysiologically characterized by ON-pathway dysfunction also showed only two sublamination peaks at IPL.

Due to the severity of the visual loss and the associated laminar changes in the retina in patients with ESCS, Jacobson et al. [17] suggested five stages of this disease. Stage I would represent congenital laminopathy, in which some of the layers are abnormally thick and there is supernormal S-cone function and normal L-cone function. Stages II–IV represent the progressive aspects of retinal remodeling and degeneration, which end at stage IV with the delaminated retina and no measurable function. According to the spectrum of structural and functional abnormalities, three of the patients in our group would be classified into stage II or III, while the fourth patient would not fit into any of these sub-categories. This fourth patient showed normal visual acuity and possible signs of L-cone and M-cone function, but the full-field ERGs revealed that retinal function was almost extinguished. It is therefore more likely that the initial stage I might include a broader spectrum of abnormalities than those suggested by Jacobson et al. [17]. Our example for probably broader congenital anomalies was seen in the brothers (ESCS-2 and

ESCS-3), who shared the same *NR2E3* mutation (c.481delA homozygous mutation [8]). Interestingly, there were functional and structural differences in their post-photoreceptor connectivity. It therefore appears that sharing this same genotype does not necessarily lead to the same phenotypic expression. Related findings have been noted previously, as patients with the same ethnic origin and homozygous for the same *NR2E3* mutation can manifest variable fundoscopic and ERG phenotypes [31]. A primarily photoreceptor pathology caused by an *NR2E3* mutation might therefore manifest itself as a wide spectrum of abnormal post-photoreceptor connectivity, which has yet to be established.

In conclusion, the spectrum of functional and structural abnormalities of the retina of patients with ESCS is wide, although there are common findings of pathognomonic changes in the full-field ERG and a predominance of S-cone activity, together with thickening of the ONL, which was identified using SD-OCT. The presence of abnormal OFF-pathway activity, which might occur in correlation with structural alterations at the level of the IPL, raises the need for further investigations of the structural–functional correlates in larger groups of patients with ESCS.

Acknowledgments The authors are grateful to Mrs. Marija Jesenšek and Mrs. Ana Jeršin, who were involved in the clinical ERG recording. This study was supported by the Slovenian Research Agency, Grant No. P3-0333. All of the authors certify that they have no affiliations with or involvement in any organization or entity with any financial interest, or non-financial interest, in the subject matter or materials discussed in this manuscript.

References

- Jacobson SG, Marmor MF, Kemp CM, Knighton RW (1990) SWS (blue) cone hypersensitivity in a newly identified retinal degeneration. *Invest Ophthalmol Vis Sci* 31:827–838
- Marmor MF, Jacobson SG, Foerster MH et al (1990) Diagnostic clinical findings of a new syndrome with night blindness, maculopathy, and enhanced S cone sensitivity. *Am J Ophthalmol* 110:124–134
- Kobayashi M, Takezawa S, Hara K et al (1999) Identification of a photoreceptor cell-specific nuclear receptor. *Proc Natl Acad Sci USA* 96:4814–4819
- Haider NB, Jacobson SG, Cideciyan AV et al (2000) Mutation of a nuclear receptor gene, *NR2E3*, causes enhanced S cone syndrome, a disorder of retinal cell fate. *Nat Genet* 24:127–131
- Schorderet DF, Escher P (2009) *NR2E3* mutations in enhanced S-cone sensitivity syndrome (ESCS), Goldmann-Favre syndrome (GFS), clumped pigmentary retinal degeneration (CPRD), and retinitis pigmentosa (RP). *Hum Mutat* 30:1475–1485
- Milam AH, Rose L, Cideciyan AV et al (2002) The nuclear receptor *NR2E3* plays a role in human retinal photoreceptor differentiation and degeneration. *Proc Natl Acad Sci USA* 99:473–478
- Sharon D, Sandberg MA, Caruso RC et al (2003) Shared mutations in *NR2E3* in enhanced S-cone syndrome, Goldmann-Favre syndrome, and many cases of clumped pigmentary retinal degeneration. *Arch Ophthalmol* 121:1316–1323
- Audo I, Michaelides M, Robson AG et al (2008) Phenotypic variation in enhanced S-cone syndrome. *Invest Ophthalmol Vis Sci* 49:2082–2093
- Marmor MF (1989) Large rod-like photopic signals in a possible new form of congenital night blindness. *Doc Ophthalmol* 71:265–269
- Udar N, Small K, Chalukya M et al (2011) Developmental or degenerative-*NR2E3* gene mutations in two patients with enhanced S cone syndrome. *Mol Vis* 17:519–525
- Lam BL, Goldberg JL, Hartley KL et al (2007) Atypical mild enhanced S-cone syndrome with novel compound heterozygosity of the *NR2E3* gene. *Am J Ophthalmol* 144:157–159
- Kinori M, Pras E, Kolker A et al (2011) Enhanced S-cone function with preserved rod function: a new clinical phenotype. *Mol Vis* 17:2241–2247
- Marmor MF, Tan F, Sutter EE, Bearse MA (1999) Topography of cone electrophysiology in the enhanced S cone syndrome. *Invest Ophthalmol Vis Sci* 40:1866–1873
- Román AJ, Jacobson SG (1991) S cone-driven but not S cone-type electroretinograms in the enhanced S cone syndrome. *Exp Eye Res* 53:685–690
- Miyake Y (ed) (2006) Enhanced S-cone syndrome. In: *Electrodiagnosis of retinal diseases*. Springer, Tokyo, pp 68–71
- Gouras P (2003) The role of S-cones in human vision. *Doc Ophthalmol* 106:5–11
- Jacobson SG, Sumaroka A, Aleman TS et al (2004) Nuclear receptor *NR2E3* gene mutations distort human retinal laminar architecture and cause an unusual degeneration. *Hum Mol Genet* 13:1893–1902
- Hayashi T, Kitahara K (2005) Optical coherence tomography in enhanced S-cone syndrome: large macular retinoschisis with disorganized retinal lamination. *Eur J Ophthalmol* 15:643–646
- Park SP, Hong IH, Tsang SH et al (2013) Disruption of the human cone photoreceptor mosaic from a defect in *NR2E3* transcription factor function in young adults. *Graefes Arch Clin Exp Ophthalmol* 251:2299–2309
- Cima I, Breclj J, Sustar M et al (2012) Enhanced S-cone syndrome with preserved macular structure and severely depressed retinal function. *Doc Ophthalmol* 125:161–168
- Sustar M, Hawlina M, Breclj J (2011) Electroretinographic evaluation of the retinal S-cone system. *Doc Ophthalmol* 123:199–210
- Beharic A, Stirn-Kranjc B, Breclj J (2012) Electrophysiological assessment of the retina in children with congenital nystagmus. *Zdr Vest* 81:73–82
- Sustar M, Stirn-Kranjc B, Breclj J (2012) Children with complete or incomplete congenital stationary night

- blindness: ophthalmological findings, standard ERGs and ON-OFF ERGs for differentiation between the types. *Zdr Vest* 81:16–28
24. Hawlina M, Konec B (1992) New noncorneal HK-loop electrode for clinical electroretinography. *Doc Ophthalmol* 81:253–259
 25. Hood DC, Bach M, Brigell M et al (2012) ISCEV standard for clinical multifocal electroretinography (mfERG) (2011 edition). *Doc Ophthalmol* 124:1–13
 26. Marmor MF, Fulton AB, Holder GE et al (2009) ISCEV Standard for full-field clinical electroretinography (2008 update). *Doc Ophthalmol* 118:69–77
 27. Barthelmes D, Gillies MC, Sutter FKP (2008) Quantitative OCT analysis of idiopathic perifoveal telangiectasia. *Invest Ophthalmol Vis Sci* 49:2156–2162
 28. Barthelmes D, Sutter FK, Kurz-Levin MM et al (2006) Quantitative analysis of OCT characteristics in patients with achromatopsia and blue-cone monochromatism. *Invest Ophthalmol Vis Sci* 47:1161–1166
 29. Hood DC, Cideciyan AV, Roman AJ, Jacobson SG (1995) Enhanced S cone syndrome: evidence for an abnormally large number of S cones. *Vision Res* 35:1473–1481
 30. Greenstein VC, Zaidi Q, Hood DC et al (1996) The enhanced S cone syndrome: an analysis of receptor and post-receptor changes. *Vis Res* 36:3711–3722
 31. Bandah D, Merin S, Ashhab M et al (2009) The spectrum of retinal diseases caused by NR2E3 mutations in Israeli and Palestinian patients. *Arch Ophthalmol* 127:297–302
 32. Iannaccone A, Fung KH, Eyestone ME, Stone EM (2009) Treatment of adult-onset acute macular retinoschisis in enhanced S-cone syndrome with oral acetazolamide. *Am J Ophthalmol* 147:307–312
 33. Pachydaki SI, Klaver CC, Barbazetto IA et al (2009) Phenotypic features of patients with NR2E3 mutations. *Arch Ophthalmol* 127:71–75
 34. Bush RA, Sieving PA (1994) A proximal retinal component in the primate photopic ERG a-wave. *Invest Ophthalmol Vis Sci* 35:635–645
 35. Sieving PA (1993) Photopic ON- and OFF-pathway abnormalities in retinal dystrophies. *Trans Am Ophthalmol Soc* 91:701–773
 36. Sieving PA, Murayama K, Naarendorp F (1994) Push-pull model of the primate photopic electroretinogram: a role for hyperpolarizing neurons in shaping the b-wave. *Vis Neurosci* 11:519–532
 37. Ueno S, Kondo M, Ueno M et al (2006) Contribution of retinal neurons to d-wave of primate photopic electroretinograms. *Vis Res* 46:658–664
 38. Evers HU, Gouras P (1986) Three cone mechanisms in the primate electroretinogram: two with, one without off-center bipolar responses. *Vis Res* 26:245–254
 39. Tanna H, Dubis AM, Ayub N et al (2010) Retinal imaging using commercial broadband optical coherence tomography. *Br J Ophthalmol* 94:372–376
 40. Famiglietti EV, Kolb H (1976) Structural basis for ON- and OFF-center responses in retinal ganglion cells. *Science* 194:193–195
 41. Nelson R, Famiglietti EV, Kolb H (1978) Intracellular staining reveals different levels of stratification for on- and off-center ganglion cells in cat retina. *J Neurophysiol* 41:472–483